An Acad Bras Cienc (2024) 96(Suppl. 1): e20231231 DOI 10.1590/0001-3765202420231231
Anais da Academia Brasileira de Ciências | *Annals of the Brazilian Academy of Sciences*
Printed ISSN 0001-3765 I Online ISSN 1678-2690
www.scielo.br/aabc | www.fb.com/aabcjournal

ANIMAL SCIENCE

Patterns of allometric and heterochronic changes in the early ontogeny of species of *Physalaemus* (Anura: Leptodactylidae)

MARIANNA ISABELLA R.R. DE OLIVEIRA, JIMENA GROSSO, MARCELO F. NAPOLI, LUIZ N. WEBER & FLORENCIA VERA CANDIOTI

Abstract: We studied the relationship between shape, size, and developmental time in the embryonic ontogeny of 15 species of the frog genus *Physalaemus*. As in other anuran exotrophic embryos, shape changes are correlated with size increase and mainly concern tail elongation, decrease in body height, and increase in fin height. Size ranges and developmental times vary interspecifically. Embryos of the *P. signifer* Clade and the *P. gracilis* Group are among the largest, are slightly peramorphic, and develop fast regarding congeneric species. Embryos of *P. cicada* combine the smallest sizes with fast development and the most peramorphic shapes. The paedomorphic shapes of embryos of *P. biligonigerus* and *P. henselii* groups are correlated with fast vs. slow developmental times respectively. Trajectories in the *P. cuvieri* Group are diverse and in general differ in size and developmental time. The embryos of *P. cristinae* and from the Argentinean lineage of *P. cuvieri* stand out with the longest development. Sequences of developmental events are overall conserved in the genus, and main differences concern mouthpart ontogeny. This study constitutes the first attempt to evaluate morphological, allometric, and heterochronic parameters of the early ontogeny of anurans and how these can vary and contribute to diversification in taxonomic groups.

Key words: geometric morphometrics, development, sequence heterochrony, shape, size.

INTRODUCTION

Comparative studies have emphasized the great structural and temporal variation in the early ontogeny of anurans (e.g., Richardson et al. 1997, Chipman et al. 2000, Vera Candioti et al. 2016, Grosso et al. 2019, Chuliver & Fabrezi 2019). These studies highlighted the neglected potential of embryonic phases in revealing significant aspects of the anurans' evolutionary history.

A significant part of organisms' morphological variation is related to size changes during growth and constitutes the field study of allometry (e.g., Gould 1966). From a multivariate approach, allometry is defined as the dependence of shape on size and involves covariation between morphological characters (e.g., Klingenberg 2016). Closely related species may differ in allometric patterns (e.g., Wilson & Sánchez-Villagra 2009), and therefore, it is important to analyze and compare their ontogenetic trajectories because they may reflect the evolutionary change in growth patterns (Klingenberg et al. 2010). In anurans, the contribution of allometry to morphological change has been investigated for many taxa using traditional approaches (e.g., linear measurements; Lima & Pederassi 2012). Geometric morphometric tools are helpful in this type of investigation because they can detect most subtle variations and allow the interpretation of shape and size separately. Accordingly, they have been applied in studies

on anuran larval and postmetamorphic development (e.g., Larson 2002, 2004, 2005, Ponssa & Vera Candioti 2012, Duport-Bru et al. 2019). Studies on the role of allometric changes in the initial ontogeny are practically nonexistent in frogs, being known only for treefrogs of the genus *Boana* (Navarro Acosta & Vera Candioti 2017).

Allometry is directly linked to heterochrony, a fundamental concept in evolutionary biology that relates ontogeny and phylogeny (reviewed in Klingenberg 1998). In its classical definition (Gould 1977, Alberch et al. 1979), the concept explicitly incorporates time as an independent variable, although size is used as a time surrogate in several approaches. In this context, patterns of paedomorphosis and peramorphosis can be explained by shape-size-time relationships. An alternative approach to the study of heterochrony was proposed by Smith (2001) and termed "sequence heterochrony" as opposed to "growth heterochrony" applied to the former approach. Neither time, shape, or size are explicitly considered, but heterochronic changes are inferred from transformations in the order of occurrence of developmental events.

In this work we studied embryos of 15 species of Neotropical foam frogs *Physalaemus*. This genus is currently composed of 50 species (Frost 2023), distributed in two major clades (sensu Lourenço et al. 2015): the *P. signifer* Clade (19 spp.) that includes the *P. signifer* and *P. deimaticus* phenetic groups, *P. araxa* and *P. nattereri*; the *P. cuvieri* Clade with *P. biligonigerus* Group (4 spp.), *P. cuvieri* Group (9 spp.), *P. henselii* Group (2 spp.), *P. gracilis* Group (6 spp.), *P. olfersii* Group (7 spp.), *P. cicada*, and *P. aguirrei*; plus *P. atim* not assigned to clade. The initial ontogeny of *Physalaemus* has been explored in recent studies (Vera Candioti et al. 2011, Gómez et al. 2016, Chuliver & Fabrezi 2019, Oliveira et al. 2022). A complete approach framed in an explicit phylogenetic context was presented by Grosso et al. (2019), who explored the evolutionary transformations related to temporal changes in developmental sequences of embryonic characteristics of Leiuperinae, among them 11 species of the *P. cuvieri* Clade.

Intending to explore the role of allometry and heterochrony in the generation of variation in embryonic phases of *Physalaemus*, our main goals were: (1) to compare shape-size relationships to interpret patterns of allometric changes; (2) to compare shape-developmental time relationships to interpret patterns of growth heterochrony; and (3) to explore heterochronic variations in sequences of developmental events. This integrative approach will serve as a basis to explore the evolution of early ontogeny in these frogs, complementing previous contributions to embryonic morphological features in the genus.

MATERIALS AND METHODS

Specimens and embryonic series

We analyzed embryonic series of 15 species of *Physalaemus* representing the two main clades of Lourenço et al. (2015). The list of species and pertinent information are given in Table I and include: (1) *P. cuvieri* Clade: *P. albifrons*, *P. albonotatus*, *P. cristinae*, *P. cuvieri*, *P. erikae* (from *P. cuvieri* Group); *P. biligonigerus*, *P. riograndensis*, *P. santafecinus* (from *P. biligonigerus* Group); *P. fernandezae*, *P. henselii* (from *P. henselii* Group); *P. carrizorum*, *P. gracilis* (from *P. gracilis* Group); *P. cicada* (not assigned to Group); and (2) *P. signifer* Clade: *P. camacan*, *P. signifer*. As outgroup, we included the ontogenetic trajectory of a representative of the sister genus of *Physalaemus*, the leiuperine *Pleurodema borellii*. Most embryos were available from previous studies (Grosso et al. 2019, Oliveira et al. 2022), and new ontogenetic series were constructed for *P. erikae* and a lineage of *P. cuvieri* from Brazil.

Table I. Material examined, indicating collection data, number of specimens analyzed, and ranges of size increase (in centroid size units CS) and developmental time (in hours after oviposition HO).

***Physalaemus biligonigerus* Group**
P. biligonigerus (Cope, 1861) – Argentina, Chaco, General Güemes: 27.5 kilometers southeast to Misión Nueva Pompeya (LGE 11847). n = 101, CS 0.71–0.85, HO 48–102.
P. riograndensis Milstead, 1960 – Argentina, Misiones, near to Profundidad (LGE 7200). n = 23, CS 0.68–0.88, HO 36–72.
P. santafecinus Barrio, 1965 – Argentina, Corrientes, Ituzaingó (LGE 7005). n = 64, CS 0.69–0.90, HO 60–108.
***Physalaemus cuvieri* Group**
P. albifrons (Spix, 1824) – Brazil, Bahia, Brotas de Macaúbas (UFSB512); n = 59, CS 0.74–0.89, HO 36–80.
P. albonotatus (Steindachner, 1864) – Argentina, Jujuy, Calilegua (FML 29516); n = 10, CS 0.74–0.88, HO 48–84.
P. cristinae Cardozo, Tomatis, Duport-Bru, Kolenc, Borteiro, Pansonato, Confalonieri, Lourenço, Haddad & Baldo, 2023 – Argentina, Corrientes, Ituzaingó (LGE 7004); n = 62, CS 0.76–0.92, HO 84–178.
P. cuvieri Fitzinger, 1826 – Argentina, Misiones, Eldorado, Santiago de Liniers, Reserva Natural La Emilia, Establecimiento Don Guillermo (LGE 7074); n = 51, CS 0.81–0.96, HO 78–120. Brasil, Bahia, Barreiras (UFSB513); n = 49, CS 0.76–0.89, HO 36–80.
P. erikae Cruz & Pimenta, 2004 – Brazil, Bahia, Porto Seguro (UFSB514); n = 31, CS 0.70–0.90, HO 40–64.
***Physalaemus gracilis* Group**
P. carrizorum Cardozo & Pereyra, 2018 – Argentina, Misiones, San Pedro, Parque Provincial El Piñalito (LGE 20430); n = 24, CS 0.79–0.97, HO 36–86.
P. gracilis (Boulenger, 1883) – Uruguay, Montevideo, Parque Vaz Ferreira (LGE 1797); n = 5, CS 0.87–0.96, HO not available.
***Physalaemus henselii* Group**
P. fernandezae (Müller, 1926) – Argentina, Buenos Aires, Ensenada, Punta Lara (LGE 1794); n = 7, CS 0.82–0.89, HO 108–144.
P. henselii (Peters, 1872) – Uruguay, Rocha, Ruta N° 10, km 255 (LGE 1795); n = 22, CS 0.83–0.90, HO not available.
Not assigned to Group
P. cicada Bokermann, 1966 – Brazil, Bahia, Brotas de Macaúbas (UFSB511); n = 49, CS 0.69–0.85, HO 36–80.
***Physalaemus signifer* Clade**
P. camacan Pimenta, Cruz & Silvano, 2005 – Brazil, Bahia, Itabuna, Campus da UESC (UFSB517); n = 45, CS 0.84–0.98, HO 48–78.
P. signifer (Girard, 1853) – Brazil, Bahia, Porto Seguro (UFSB515); n = 68, CS 0.81–1.01, HO 36–84.
Outgroup
Pleurodema borellii (Peracca, 1895) – Argentina, Tucumán, Fundación Miguel Lillo (LGE 6226); n = 6, CS 0.83–0.96, HO 58–80.

For the construction of these series, clutches were collected in the field and from amplectant pairs under permission of national and regional authorities (collecting permit, ICMBio 60078-1, authentication number 54917396, www.icmbio.gov.br/Sisbio; animal ethics committee, CEUA/UFBA 43/2017). The specimen manipulation follows the recommendations of the CEUA-MNHN protocol (Res. 1/2019). Species identity was confirmed by identifying amplectant

pairs, vocalization, and rearing tadpoles to metamorphosis. The clutches were maintained in containers with dechlorinated water under seminatural conditions, with ambient photoperiod and temperature; embryos were periodically euthanized (ca. 5 at a time) in water with lidocaine and preserved in 4% formalin every 4 to 8 hs, following Vera Candioti et al. (2016) and Grosso et al. (2017).

Allometric and heterochronic trajectories: shape, size and time

We applied landmark-based geometric morphometrics to characterize shape changes of embryos during early ontogeny. Ontogenetic trajectories were defined between comparable stages: the pigmentation of the eye (about Stage 21; Gosner 1960) was considered the beginning of the trajectory (onset), and the concealing of the right gill (Stage 24) as the end (offset). This interval was selected because younger embryos have a kyphotic or lateral curvature that affects standardization of position, and later stages show little or no significant shape change with size increasing and/or developmental time. A total of 676 embryos were processed for analysis. Specimens were observed and photographed in lateral view with an image analyzer coupled to a LeicaEZ4 stereomicroscope. We digitized 20 landmarks on the body side and tail using TpsDig2 2.3 version (Rohlf 2005). Landmark selection followed Navarro Acosta & Vera Candioti (2017), redefining some points if necessary (landmarks with ambiguous location were not used and additional points in the ventral body and fins were defined; Fig. 1). Generalized Procrustes Analysis (GPA) was performed to obtain a matrix of shape (Procrustes) coordinates, where all variations related to the position, orientation, and absolute size are removed. To explore the main patterns of shape variation within and between species, we performed a principal component analysis on the covariance matrix of shape coordinates and retained the first three principal components for interpretation.

We followed the approach by Strelin et al. (2016) and Esquerré et al. (2017) to investigate the relationship between shape variation and size and developmental time increase during ontogeny. The centroid size (CS) was used as a size descriptor (Rohlf & Bookstein 1990), and its log-transformed value (logCS) was used in subsequent steps. To study allometric variations (i.e., shape-size relationships), we first performed multivariate regressions of shape coordinates on logCS. This procedure tests the existence of allometric growth against the null hypothesis of isometric development and provides a percentage of the total variation in shape as a function of size. For growth heterochrony studies (i.e., shape-developmental time relationships), developmental time was recorded for each preserved embryo and expressed as "hours after oviposition". Unfortunately, developmental time data were unavailable for *P. gracilis* and *P. henselii*, so these two species had to be excluded from these analyses. The variation of shape on developmental time was explored similarly to the analysis of shape on size variation, using the hours after oviposition as the independent variable in multivariate regressions. Visualizations of shape-size and shape-developmental time relationships were provided by scatterplots of regression scores (Mitteroecker et al. 2013) against logCS and hours after oviposition. All analyses and plots in this work were performed using the MorphoJ software (Klingenberg 2011).

Sequence heterochrony: developmental events

To complement the former approach, we applied sequence heterochrony analysis (Smith 2001) to our full set of species. This includes species already covered in Grosso et

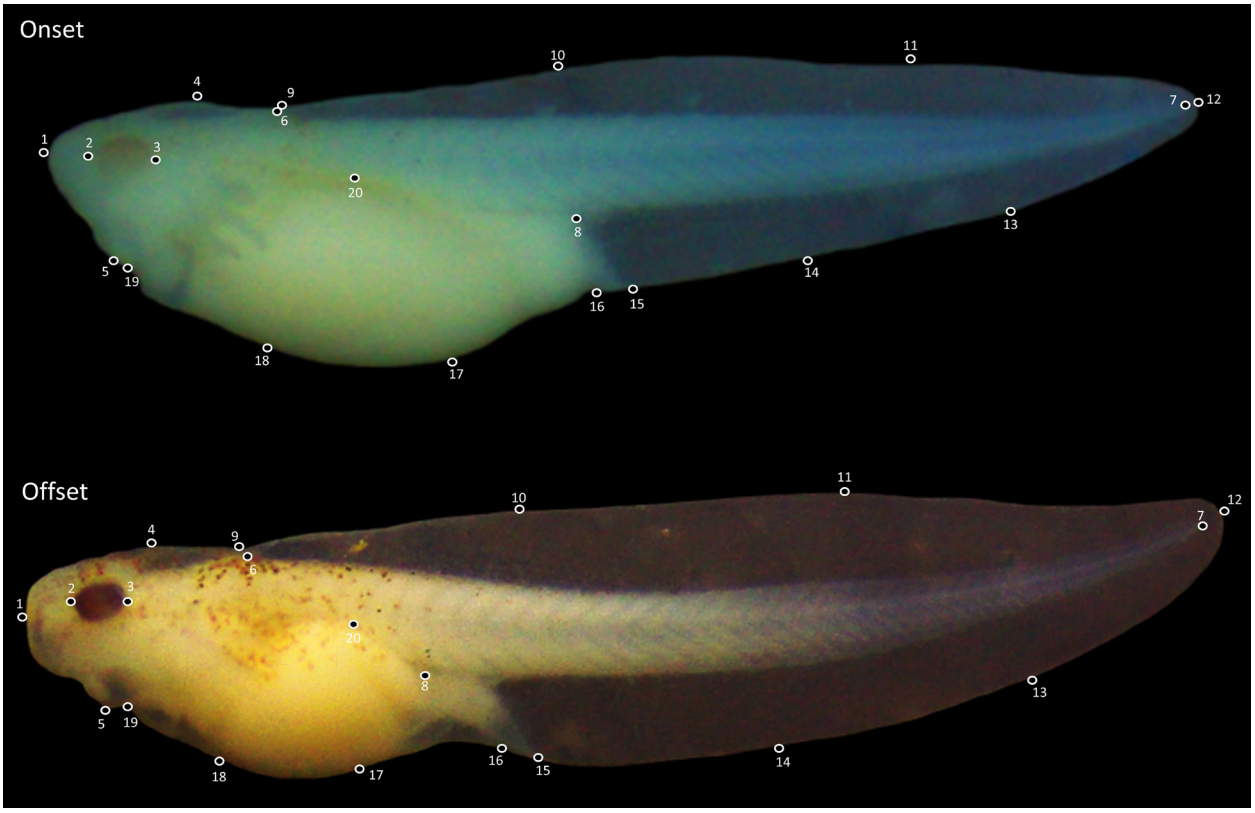

Figure 1. Landmark configurations for geometric morphometric analysis of embryos of *Physalaemus*, shown on examples of onset and offset shapes. 1 maximum curvature of the snout, 2 anterior margin of the eye, 3 posterior margin of the eye, 4 maximum body height, 5 adhesive gland tip, 6 dorsal junction of the caudal musculature and body, 7 extreme of the caudal musculature, 8 ventral junction of the caudal musculature and body, 9 origin of the dorsal fin, 12 tail fin tip, 15 distal margin of the vent tube, 16 proximal margin of the vent tube, 19 base of the adhesive gland, 20 most anterior point of the axis separating caudal myotomes. Points 10 and 11 are equidistant between landmarks 9 and 12, 13 and 14 equidistant between 12 and 15, and 17 and 18 equidistant between 16 and 19.

al. (2019), and we added the developmental sequences of *Physalaemus camacan*, *P. erikae*, *P. signifer*, and the lineage of *P. cuvieri* from Brazil (Supplementary Material - Table SI). We analyzed a segment of the trajectory from the tailbud stage to the appearance of the hind limbs, and we considered 24 events related to the ontogeny of embryonic and larval structures (Supplementary Material - Figure S1): adhesive glands: AG adhesive gland first visible, AGA adhesive glands absent; gills: 1G first gill pair bud, 1GB first gill pair branched, 2G second gill pair bud, 2GB second gill pair branched, GFD gills at full development, OB operculum at gill base, OM operculum medially fused, RGC right gill covered by operculum, LGC left gill covered by operculum, ES spiracle developed; hind limbs: HLB hindlimb buds, HL26 hind limbs at Gosner Stage 26; tail: TB tail bud, TL=BL tail length/body length = 1; oral disc and digestive tract: A1 labial tooth ridge A1, A2 labial tooth ridge A2, P1 labial tooth ridge P1, P2 labial tooth ridge P2, FP first marginal papillae, MP marginal papillae complete, LOD oral disc fully formed, IC first coil in digestive tract. The developmental sequences were converted into ordered ranks and compared using a two-axis graph, in which events ordered as they occur in a reference

trajectory (*Pleurodema borellii*) are plotted in relation to their rank number.

RESULTS

Shape variation

The shape variation is illustrated in the space defined by the principal components (PC) that represented the largest amount of variation, PC1 (54%), PC2 (15%), and PC3 (8%), which together explain 78% of the total variation (Fig. 2 and Table II). PC1 summarizes ontogenetic shape change, with young, less developed embryos at lower scores and more developed, larval-like embryos at higher scores. Shape transformations (transformation grids) imply mainly tail lengthening, an increase in fin height, and a reduction in body height due to the reabsorption of the vitelline mass. The PC2 and PC3 recover some interspecific variation, with

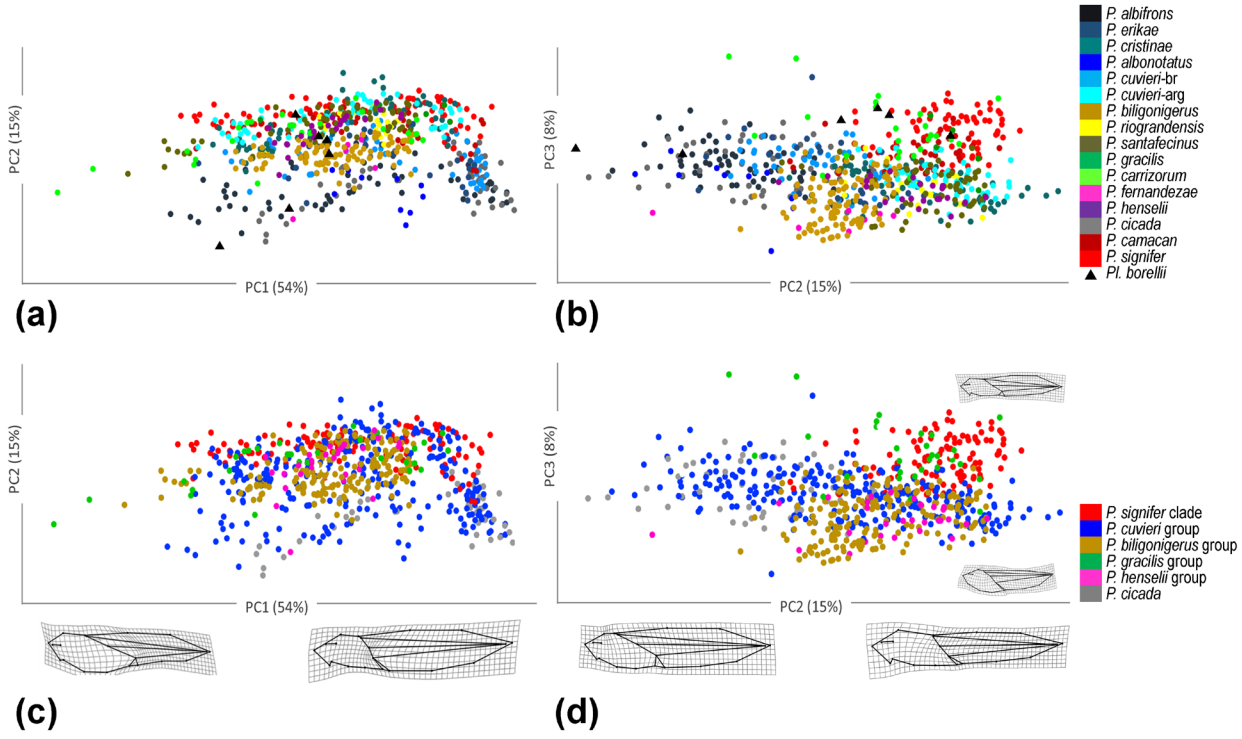

Figure 2. Shape variation in embryos of *Physalaemus*, Gosner Stages 21–24. Ordination plots of three first principal components, PC1-PC2 (a, c) and PC2-PC3 (b, d) are shown. Colors indicate individual taxa (a, b) and species groups (c, d). Line drawings show shape changes along the axes, as deformed grids compared to a rectangular grid corresponding to the consensus shape.

Table II. Results of the principal component analysis (PCA). Eigenvalues, variances, and cumulative variances are detailed for the first three principal components and summarized for the remaining axes.

Principal Component	Eigenvalue	Variance (%)	Cumulative variance (%)
1	0.0024	54.829	54.829
2	0.0007	15.3	70.22
3	0.0003	8.122	78.349
4–36	0.0002 – 0.0000	16.719	100

the main changes along PC2 explained by a shift in dorsal fin origin and along PC3 by differences in body and fin height.

The ordination generally shows a wide overlap among species in shape trajectories (Fig. 2a, b), highlighting that ontogenetic shape changes are similar in the genus. Main variations concern the species groups (Fig. 2c, d): embryos of the *P. signifer* Clade and *P. gracilis* Group have, in general, lower bodies and dorsal fins higher and more posterior, whereas *P. henselii*, *P. cicada*, and species of *P. biligonigerus* and *P. cuvieri* Groups have highest bodies, more anterior dorsal fin, and higher ventral fin. Embryos of the outgroup species *Pleurodema borellii* combine a wide variation in dorsal fin origin with intermediate values in body and fin heights.

Allometry: variations in shape-size relationship

Ranges of size increase per species are indicated in Table I. The shape change is significantly related to size increase in all *Physalaemus* species herein analyzed ($p < 0.01$), while marginally significant in *Pleurodema borellii*; percentages of variation explained by size increase are in general high (37–71%; Table III). Specific trajectories in the shape-size space are generally similar and widely overlapped in relative size range. Overall, size increase implies tail lengthening, a decrease in body height associated with yolk mass resorption, and an increase in fin height (Fig. 3a). Most species in the *P. cuvieri* Clade are smaller throughout the trajectory than those of the *P. signifer* Clade (Fig. 3b). The trajectory of *P. borellii* is similar to that of the largest *Physalaemus* species but the offset shape is less developed than those of most other species (Fig. 3a).

Embryos of the *Physalaemus signifer* Clade are the largest in our sample. The ontogenetic trajectories of *P. camacan* and *P. signifer* are mostly overlapped, although embryos of *P. signifer* tend to reach larger sizes towards the end of the trajectory (Fig. 3c). On the other hand, in the *P. cuvieri* Clade, the species groups tend to discriminate in size range, from *P. cicada* with the smallest size to species of the *P. gracilis* Group with the largest (Fig. 3d). The ontogenetic trajectories of the species from the *P. cuvieri* Group generally have intermediate sizes and shapes. The embryos of the *P. biligonigerus* and *P. henselii* Groups reach less developed offset shapes than the others; embryos of the *P. henselii* Group also show the shortest trajectories, with an overall more advanced onset shape and size (Fig. 3d).

In the clade joining *Physalaemus cicada* and *P. gracilis* and *P. biligonigerus* Groups, the species of the *P. biligonigerus* Group differ mainly in the onset shape, with embryos of *P. riograndensis* comparatively more developed; in addition, the ontogenetic trajectories of *P. santafecinus* and *P. biligonigerus* differ slightly in offset size, whereas embryos of *P. riograndensis* tend to reach a slightly less developed offset shape (Fig. 3e). The trajectory of *P. gracilis* is shorter than that of *P. carrizorum*, which in general shows less developed onset shape and size.

Finally, in the *Physalaemus cuvieri* species Group, the ontogenetic trajectories are ordered from *P. albonotatus*, with the smallest sizes, to Argentinean populations of *P. cuvieri* with the largest embryos; the remaining species overlap along intermediate sizes. In addition, the onsets and offsets of trajectories vary slightly in shape. Embryos of *P. albonotatus* generally have overdeveloped onset shapes. Embryos of *P. albifrons*, and to a lesser extent, the Brazilian population of *P. cuvieri*, have the most advanced offset shapes (Fig. 3f). Interestingly, sister taxa in the *P. cuvieri* Group differ substantially from each other in the onset shape (*P. albonotatus*

Table III. Statistical parameters and sample size from the test of allometry (H_0: Isometry) for each species.

	n	% predicted	p
Physalaemus cuvieri Clade			
Physalaemus biligonigerus Group			
P. biligonigerus	101	37.1	< 0.0001
P. riograndensis	23	52.7	< 0.0001
P. santafecinus	64	64.4	< 0.0001
Physalaemus cuvieri Group			
P. albifrons	59	61.3	< 0.0001
P. albonotatus	10	45.5	0.0021
P. cristinae	62	65.7	< 0.0001
P. cuvieri ARG	51	71.5	< 0.0001
P. cuvieri BR	49	66.6	< 0.0001
P. erikae	31	51.6	< 0.0001
P. gracilis Group			
P. carrizorum	24	67.9	< 0.0001
P. gracilis	5	48.7	< 0.0001
Physalaemus henselii Group			
P. fernandezae	7	51.4	0.0083
P. henselii	22	55.2	< 0.0001
Not assigned to Group			
P. cicada	49	54.4	< 0.0001
Physalaemus signifer Clade			
P. camacan	45	54.6	< 0.0001
P. signifer	68	68.1	< 0.0001
Outgroup			
Pleurodema borellii	6	57.7	0.0188

and *P. cristinae*), offset shape (e.g., *P. erikae* and *P. albifrons*), and embryo size (Argentinean and Brazilian lineages of *P. cuvieri*).

Growth heterochrony: variations in shape-time relationship

Developmental time values per species are indicated in Table I. Development in *Pleurodema borellii* is shorter than in most species of *Physalaemus*. Within *Physalaemus*, species differ in their trajectories in shape-time space, and shape changes associated with developmental time mainly include tail lengthening, a decrease in body height, and an increase in fin height (Fig. 4a). Embryos of the *P. signifer* Clade have very short trajectories and an early onset of shape change (Fig. 4b, c). Species in the *P. cuvieri* Clade differ widely, with embryos with early onset and rapid development and embryos with late onset

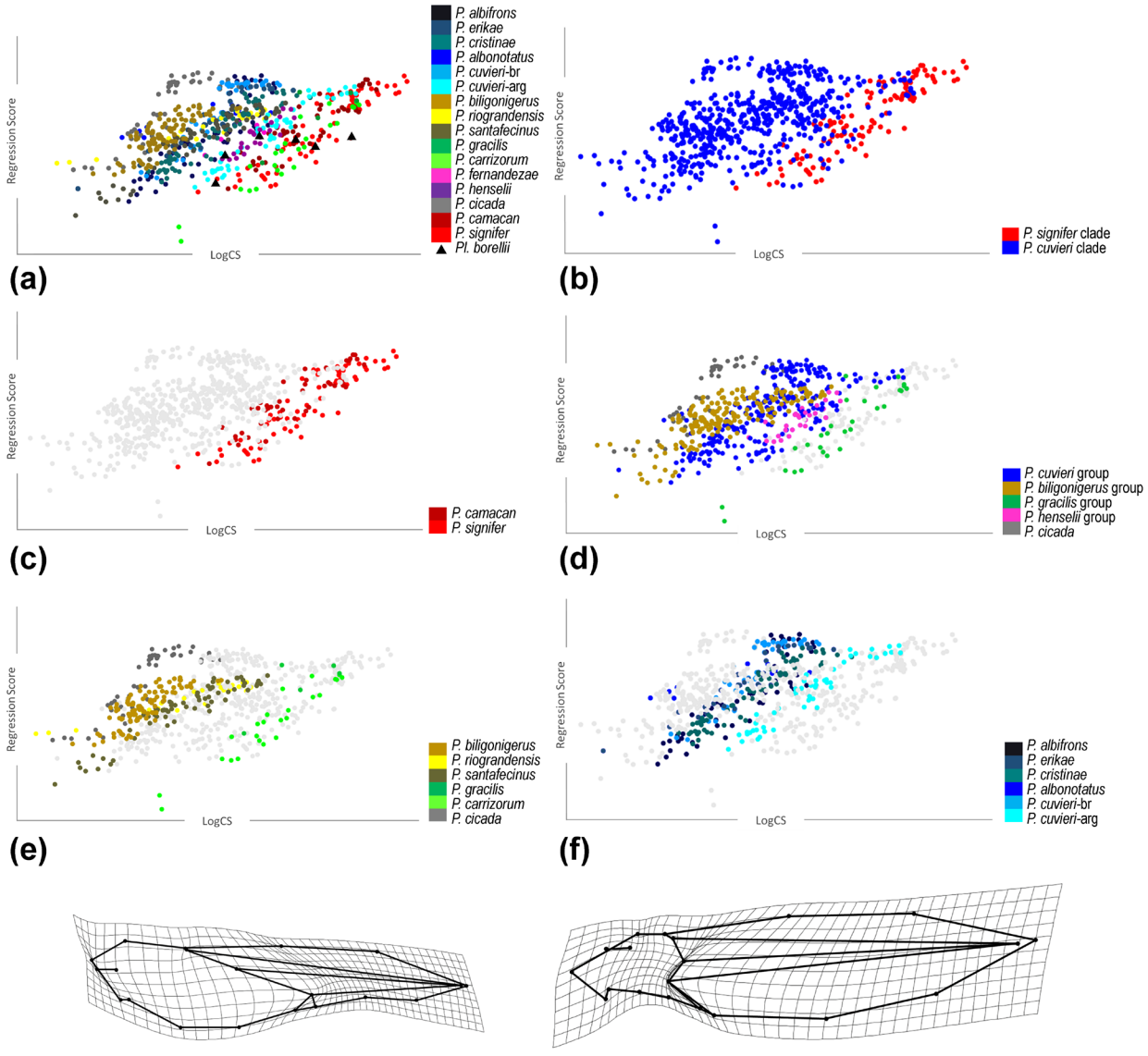

Figure 3. Allometric trajectories in embryos of *Physalaemus* (Gosner Stages 21–24). Multivariate regression of shape (summarized as regression scores) on size (logCS); species groups and species are highlighted in separate plots to facilitate interpretation. (a) Species of *Physalaemus* and *Pleurodema borellii* in comparison, (b) *P. cuvieri* and *P. signifer* Clades, (c) species of the *P. signifer* Clade, (d) species groups of the *P. cuvieri* Clade, (e) *P. cicada* plus *P. biligonigerus* and *P. gracilis* Groups, (f) *P. cuvieri* Group. Line drawings show shape changes in the smallest and largest embryos of the sample from a consensus shape (a rectangular grid).

and slow development (Fig. 4d). Regarding the *P. biligonigerus* Group, *P. riograndensis* has the shortest development, with an earlier onset and offset. *Physalaemus biligonigerus* and *P. santafecinus* differ in the rates of shape change, with *P. biligonigerus* starting shape change early and at a slower rate than *P. santafecinus*. Development in *P. carrizorum* takes intermediate time (Fig. 4e). In the *P. cuvieri* Group, three distinct patterns are revealed: most species develop fast and early (*P. albifrons*, Brazilian *P. cuvieri*, *P. erikae,* and *P. albonotatus*), embryos of *P. cuvieri* from Argentina also develop fast but starting at a later onset, and embryos of *P. cristinae* begin

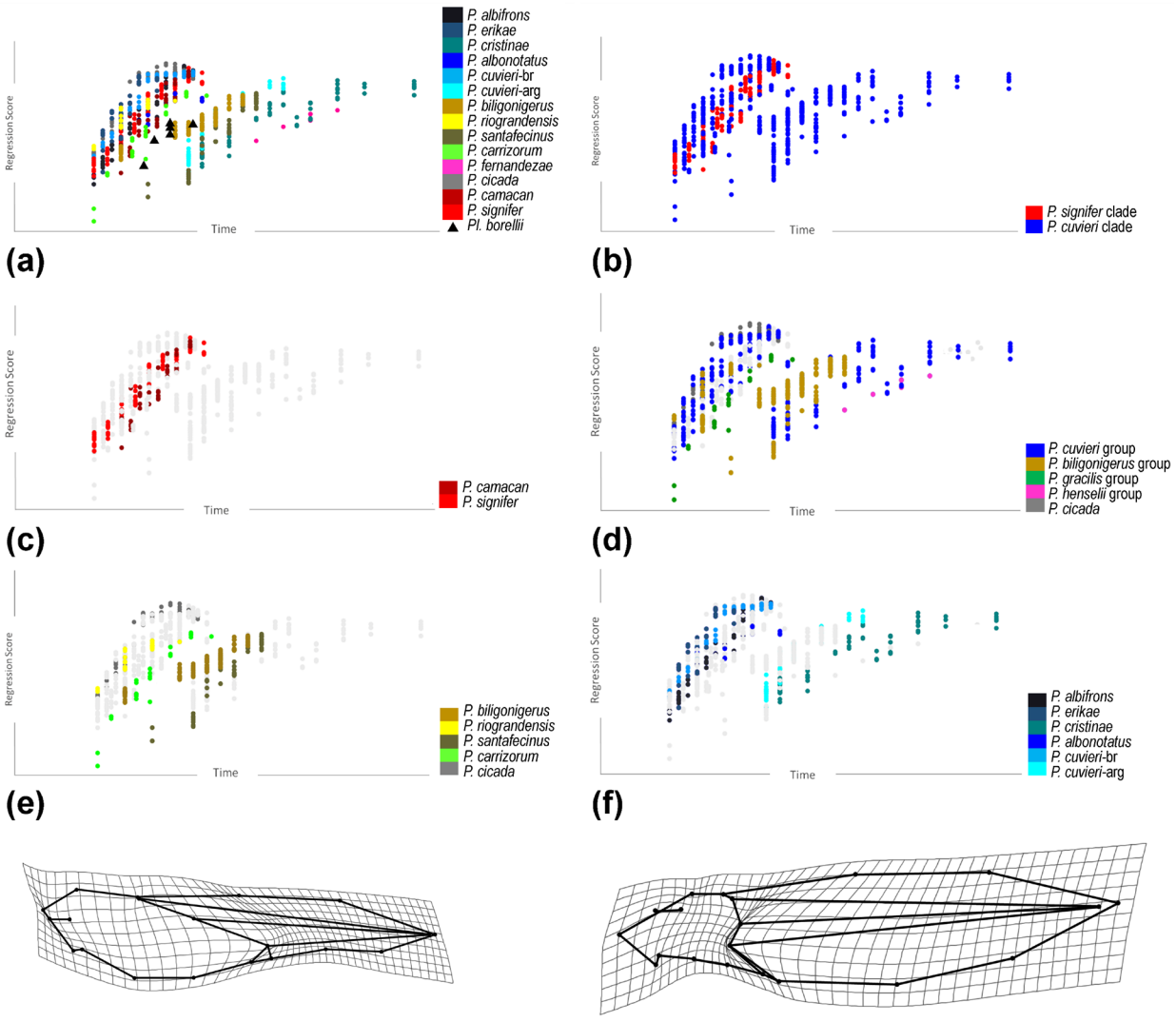

Figure 4. Growth heterochrony in embryos of *Physalaemus* (Gosner Stages 21–24). Multivariate regression of shape (summarized as regression scores) on time (hours after oviposition); species groups and species are highlighted in separate plots to facilitate interpretation. (a) Species of *Physalaemus* and *Pleurodema borellii* in comparison, (b) *P. cuvieri* and *P. signifer* Clades, (c) species of the *P. signifer* Clade, (d) species groups of the *P. cuvieri* Clade, (e) *P. cicada* plus *P. biligonigerus* and *P. gracilis* Groups, and (f) *P. cuvieri* Group. Line drawings show shape changes in the youngest and oldest embryos of the sample from a consensus shape (a rectangular grid).

shape change at approximately the same time as the latter, but the shape change rate is lower, and offset shape is acquired almost twice later (Fig. 4f).

Sequence heterochrony

The sequences of developmental events in the ontogeny of *Physalaemus* species are depicted in Figure 5. The four species we included in the analysis closely follow the pattern found by Grosso et al. (2019), with few minor differences in the developmental timing of differentiation of the operculum and spiracle and the formation of marginal papillae in the oral disc. The trajectories of *P. camacan* and *P. signifer* are similar to each other and, except for a late differentiation of the operculum, closely resemble sequences of the *P. gracilis*

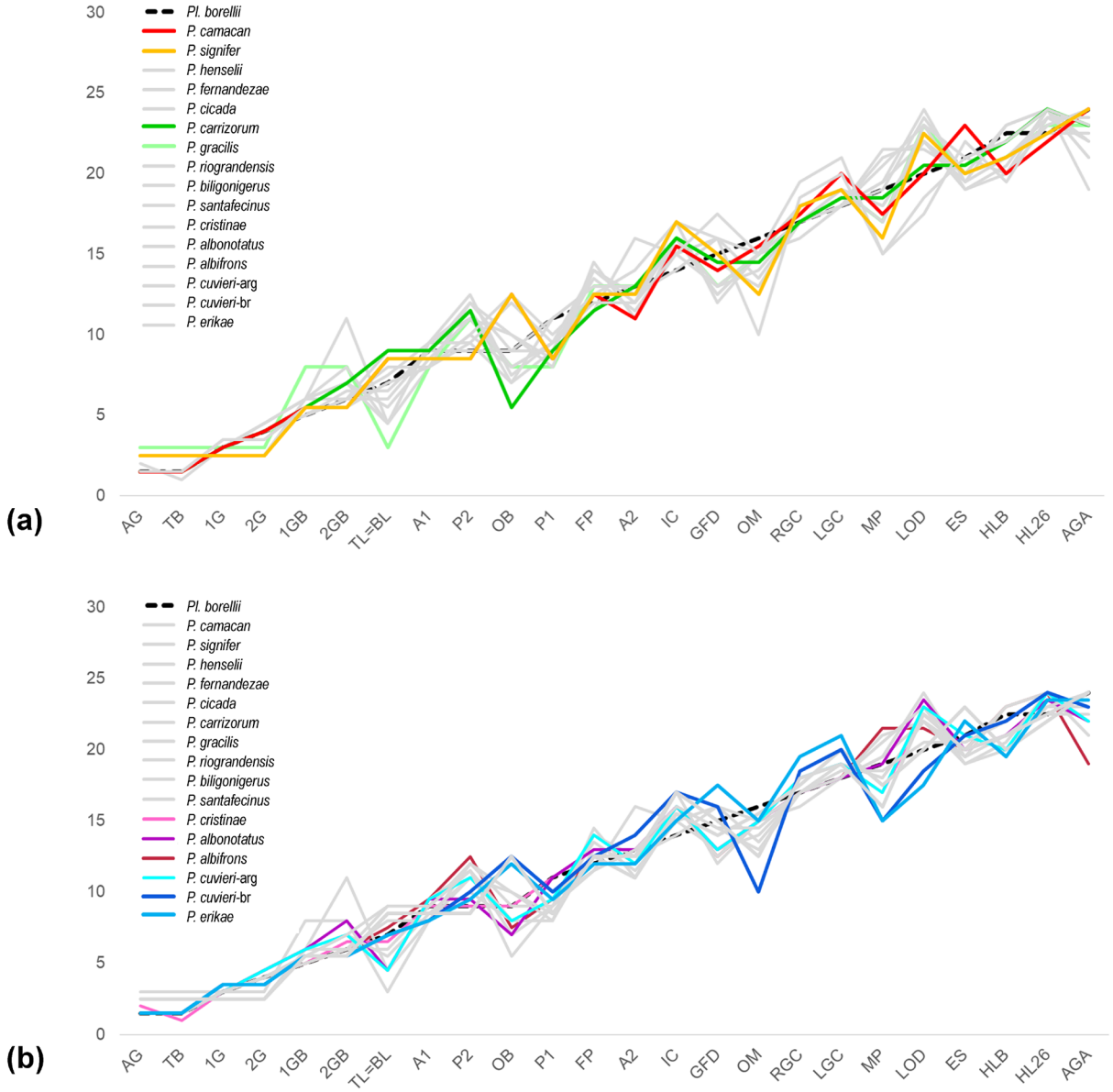

Figure 5. Sequence heterochronies in developmental trajectories of *Physalaemus*. (a) Event trajectories of *P. camacan* and *P. signifer*, as compared with species of the *P. gracilis* Group (*P. carrizorum* and *P. gracilis*) and the remaining species of the genus studied by Grosso et al. (2019; in gray), (b) trajectories of *P. erikae* and *P. cuvieri* from Brazil, as compared with species of the *P. cuvieri* Group and the remaining studied *Physalaemus* species. Developmental events: AG adhesive gland first visible, TB tail bud, 1G first gill pair bud, 2G second gill pair bud, 1GB first gill pair branched, 2GB second-gill pair branched, TL=BL tail length/body length = 1, A1 labial tooth ridge A1, P2 labial tooth ridge P2, OB operculum at gill base, P1 labial tooth ridge P1, FP first marginal papillae, A2 labial tooth ridge A2, IC first coil in digestive tract, GFD gills at full development, OM operculum medially fused, RGC right gill covered by operculum, LGC left gill covered by operculum, MP marginal papillae complete, LOD oral disc fully formed, ES spiracle developed, HLB hindlimb buds, HL26 hind limbs at Gosner Stage, AGA adhesive glands absent.

Group (Fig. 5a). Between both species, the main differences are the comparatively late medial fusion of the operculum and the formation of the spiracle in *P. camacan*. *Physalaemus erikae* and the Brazilian population of *P. cuvieri* differ in some aspects regarding other species in the

P. cuvieri Group (Fig. 5b). Both species show a delayed differentiation of the operculum and the earliest formation of marginal papillae and the whole larval oral disc. Embryos of Brazilian *P. cuvieri* are distinct in their early opercular medial fusion. Embryos of *P. erikae* stand out with the latest full development and regression of gills.

DISCUSSION

Our study evaluates different morphological parameters involved in the early ontogeny of frogs and how relationships among them can vary and evolve in closely related species. Although some results and interpretations should be taken with caution (e.g., we still lack a comprehensive sampling in the genus, some species have very small samples, and intraspecific variation is not considered), our data provide a basis to discuss the contribution of embryonic aspects to diversification in foam-nesting frogs.

Generally, the early ontogeny in most exotrophic frogs implies similar shape changes. Main transformations involve tail lengthening, a decrease in body height after yolk resorption, and an increase in fin height (e.g., Anstis 2010, Salica et al. 2011, Vera Candioti et al. 2016, Grosso et al. 2017, Chuliver & Fabrezi 2019). Within *Physalaemus*, changes along ontogeny allow us to interpret patterns of paedomorphosis and peramorphosis, by which some species end their embryonic trajectories with comparatively underdeveloped or overdeveloped shapes. In addition, some differences unrelated to ontogenetic changes allow to distinguish embryos from the *P. signifer* Clade and the *P. gracilis* Group, which generally have bodies more depressed and caudal fins lower than other species. Interspecific changes in embryo body size are noticeable, with the largest embryos of the *P. signifer* Clade being 1.5 larger than the smallest *P. cicada*. In all species, somatic growth is accompanied by rapid shape changes until gills start to regress, and after that, size growth take place without significant changes in body shape. Main transformations are later registered in punctual characters, such as regression of gills and development of the oral disc and hind limbs. A similar pattern was also reported for embryos of the treefrogs *Boana* (Navarro Acosta & Vera Candioti 2017). Developmental times also may vary widely among studied species, with an almost fourfold difference between those with faster (ca. 1 day in *Pl. borellii* and *P. erikae*) vs. slower (ca. 4 days in *P. cristinae*) development. Changes at the beginning of ontogenetic trajectories in some species imply that the initial shape changes are comparatively delayed, so that embryos spend the first hours after oviposition without experiencing fundamental transformations in shape.

As reviewed by S. J. Gould in his classical work *Ontogeny and Phylogeny* (1977), the relationship among shape, size, and time has long intrigued developmental and evolutionary biologists. In this contribution, Gould proposed a methodological frame to evaluate the correlation among those parameters between species, ideally in ancestor-descendant relationships but also between sister groups. The author also named some of the possible developmental outcomes according to which parameter (shape, size, and time) and in which direction (paedo/peramorphic, small/large, and fast/slow) the "target" species changes regarding the standard. Following this approach, we summarize our results for species of *Physalaemus*, employing the "clock model" to represent how shape change, size increase, and developmental time during the embryonic ontogeny are modified compared to the ontogenetic trajectory of *Pleurodema borellii* (Fig. 6).

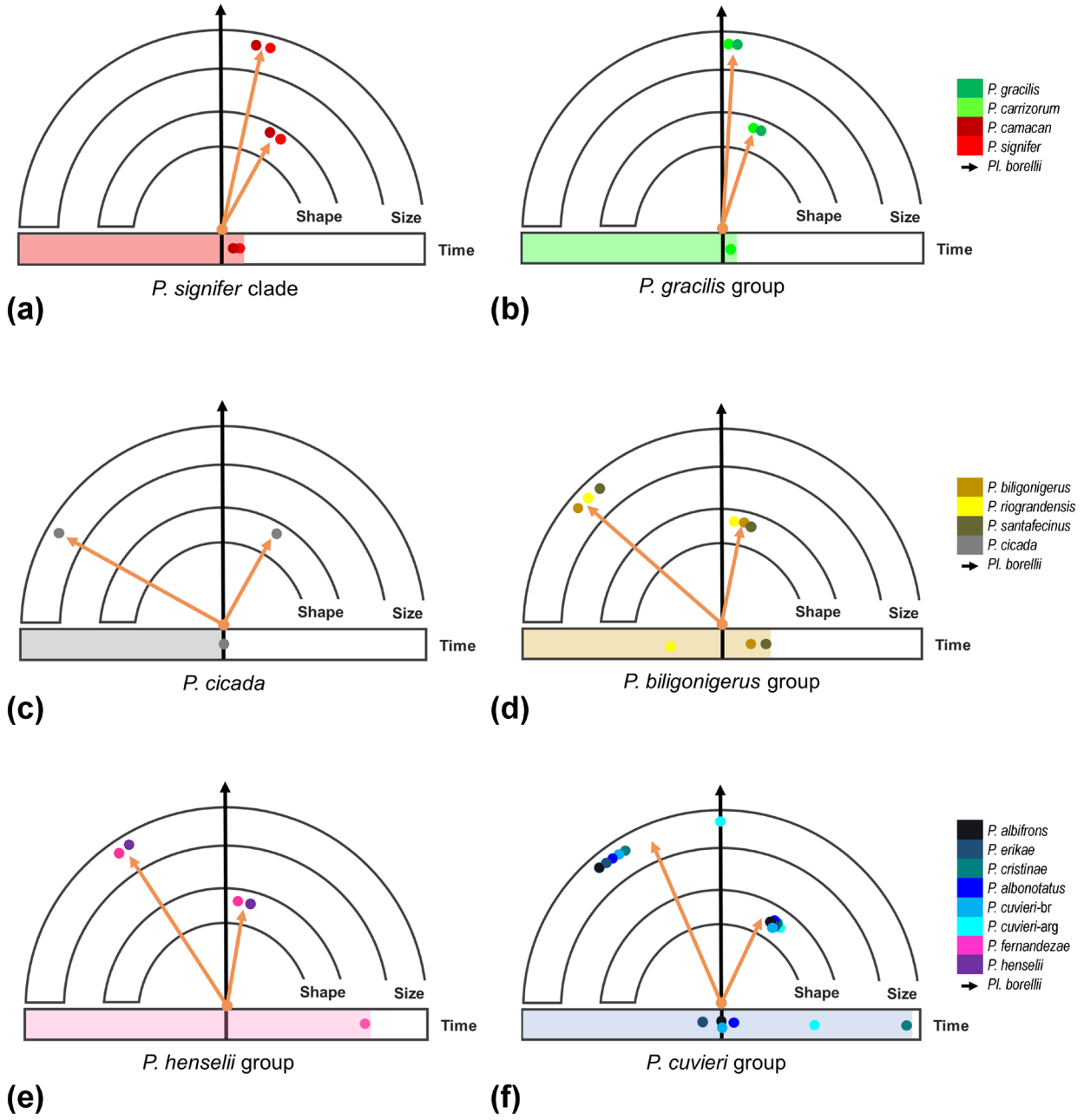

Figure 6. Shape, size, and developmental time relationships in embryos of *Physalaemus*, as compared with *Pleurodema borellii*. The "clock model" by Gould (1977) highlights changes at the offset of the trajectories (embryos at Gosner Stage 24). Species are separated into clades and groups (a-f) to facilitate visualization. The position of arrows and the length of the segment representing developmental time are estimated from regression scores (shape), LogCS (size), and hours after oviposition (time) available from analyses of allometric and heterochronic variations.

Embryos of the *Physalaemus signifer* Clade are among the largest and have a faster development regarding other species we studied (Fig. 6a). In comparison with *Pleurodema borellii*, they also have slightly peramorphic offset shapes acquired after high shape-time variation rates, corresponding to a heterochronic change type of hypermorphosis (Gould 1977). The large sizes

of eggs and embryos, typical of several species in this clade, have already been interpreted as related to the divergent reproductive modes they may exhibit (Haddad & Pombal 1998, Haddad & Prado 2005). In this view, large size and yolk provision would be essential for eggs and embryos in terrestrial foam nests that depend on being flooded or washed away to water bodies rich in food resources (Salthe & Duellman 1973, Pupin et al. 2010, 2018, Oliveira et al. 2022). Apparently, this trend is accompanied by subsequent arrestment in body growth since tadpoles and adult frogs of this group are, on the contrary, among the smallest in the genus (Weber & Carvalho-e-Silva 2001, Pimenta et al. 2005, Ruggeri & Weber 2012). The fast development of these embryos can also be related to terrestrial oviposition and, like their large size, becomes an advantage in unpredictable circumstances. Species of the *P. gracilis* Group share several features with those of the *P. signifer* Clade (Fig. 6b). Like them, they have, in general, large embryos, overdeveloped offset shapes (as compared with those of *Pleurodema*), and as hinted by *P. carrizorum*, fast development. In this case, possible interpretations related to ecological variables are subject to further investigation.

Sequences of developmental events in species of the *P. signifer* Clade generally agree with heterochronic patterns discussed in Grosso et al. (2019) for *Physalaemus*, including the early differentiation of row P1 that constitutes the main difference relative to the mouthpart ontogeny in *Pleurodema*. Disregarding a similar larval configuration, the developmental pattern of the oral disc in species of the *P. signifer* Clade and *P. gracilis* Group differs in the formation of the marginal papillae (Oliveira et al. 2022); in this context, it is interesting that the final events of oral disc formation occur slightly earlier than in most other embryos of *Physalaemus*.

On the other extreme, the embryos of *Physalaemus cicada* are the smallest in our sample and develop very fast, reaching the most peramorphic shapes (Fig. 6c). This species inhabits xeric environments, like the Brazilian Caatinga biome, and they are among the first species to be found in pounds when the reproductive season begins (Vieira & Arzabe 2008). This ecosystem has high temperatures, with daily variations even more pronounced than annual fluctuations (Bucher 1982), and temporary pounds dry up quickly. Therefore, a short development with a high shape change rate could be adaptive in these conditions.

In relation to congeneric species, embryos of the *Physalaemus biligonigerus* and *P. henselii* Groups are comparatively paedomorphic and have small to mid sizes (Fig. 6d, e). Developmental time is very short in *P. riograndensis*, whereas in *P. fernandezae,* the onset of shape change is delayed almost three times. Paedomorphosis in these species (*P. riograndensis* regarding other species of the *P. biligonigerus* Group, and *P. henselii* Group as compared with other members of the *P. cuvieri* Clade) is then explained by different processes. Whereas in *P. riograndensis* it is associated with a very fast and early development and relatively small size, in species of *P. henselii* Group paedomorphosis co-occurs with midsized embryos and seemingly a long and low-rated development at initial ontogeny previous to eye development. Paedomorphosis in body shape can be accompanied by reductions in other characters, such as the differentiation of only two lower labial ridges in the oral disc of *P. riograndensis* and only two gill pairs in species of *P. henselii* Group (Vera Candioti et al. 2011, Grosso et al. 2019). In this latter, paedomorphic features have been interpreted as related to development at low temperatures (during the winter in southern regions of South America;

Maneyro et al. 2008, Lourenço et al. 2015, Grosso et al. 2019).

Finally, the *Physalaemus cuvieri* Group shows a wide diversity of embryonic development (Fig. 6f), with ontogenetic trajectories mainly transposed in size and time values. A group of species, including *P. albonotatus*, *P. erikae*, *P. albifrons*, and Brazilian populations of *P. cuvieri*, develop fast and reach intermediate sizes. Instead, shape changes in *P. cristinae* and the Argentinean lineage of *P. cuvieri* initiate later, and development of *P. cristinae* proceeds at a lower rate. Embryos of the Argentinean lineage of *P. cuvieri* are also the largest ones in the group. The diversity of allometric and heterochronic trajectories herein observed for *P. cuvieri* supports previous studies that considered this taxon a potential species complex (Barreto & Andrade 1995, Quinderé et al. 2009, Nascimento et al. 2019).

This study constitutes the first attempt to investigate in an integrative way different aspects of embryonic ontogeny in frogs. The morphological descriptions from previous contributions is complemented by studying dynamic trajectories that consider the size and the developmental time in correlation with shape changes. A possible drawback is the integration of different approaches for heterochrony analysis. Specifically, the need to define onset and offset shapes defined by some developmental event (e.g., in our case, eye pigmentation and concealment of the right gill) may confront the fact that developmental events can show heterochronic shifts themselves (as revealed for the second example). How this impacts the analysis and interpretation of interspecific variation in developmental patterns still needs further theoretical and methodological work and is currently subject to investigation in our research group. Furthermore, a recently developed approach that considers allometric and heterochronic changes in an explicitly phylogenetic context (i.e., Catalano et al. 2019, 2021, M.I.R.R. Oliveira et al. unpublished data) will allow reinterpreting the evolution of developmental patterns in leiuperine embryos.

Acknowledgments

This study was financially supported by Fundação de Amparo à Pesquisa do Estado da Bahia (FAPESB; Nº BOL0459/2017), Agencia Nacional de Promoción de la Investigación, el Desarrollo Tecnológico y la Innovación (PICT 2017–2437 and 2018–3349), and FONDECYT Postdoctorado 2020 N° 3200490 to J. Grosso. Specimens were collected under permit number 60078–3 SISBIO (Código de autenticação: 0600780320181101). We sincerely thank the staff of Laboratório de Taxonomia e História Natural de Anfíbios (AMPHIBIA) from the Universidade Federal da Bahia (UFBA) and Laboratório de Ecologia e Zoologia from the Universidade Federal do Sul da Bahia (UFSB) for logistical support. MFN acknowledges the Conselho Nacional de Desenvolvimento Científico e Tecnológico (CNPq) for productivity grants (#310490/2018-9 and #314496/2021-1).

REFERENCES

ALBERCH P, GOULD SJ, OSTER GF & WAKE DB. 1979. Size and shape in ontogeny and phylogeny. Paleobiology 5: 296-317.

ANSTIS MA. 2010. Comparative study of divergent embryonic and larval development in the Australian frog genus *Geocrinia* (Anura: Myobatrachidae). Rec West Aust Mus 25: 399-440.

BARRETO LN & ANDRADE GV. 1995. Aspects of the reproductive biology of *Physalaemus cuvieri* (Anura: Leptodactylidae) in northeastern Brazil. Amphibia-Reptilia 16: 67-76.

BUCHER EH. 1982. Chaco and Caatinga – South American arid savannas, woodlands and thickets. In: Huntey BJ & Walther BH (Eds), Ecology of tropical savannas. Berlin and Heidelberg: Springer Verlag, p. 48-79.

CATALANO S, SEGURA V & VERA CANDIOTI F. 2019. PASOS: a method for the phylogenetic analysis of shape ontogenies. Cladistics 35: 671-687.

CATALANO S, SEGURA V & VERA CANDIOTI F. 2021. SPASOS v.1.0: a program for the inference of ancestral shape ontogenies. Cladistics 37: 630-638.

CHIPMAN AD, HAAS A, TCHERNOV E & KHANER O. 2000. Variation in anuran embryogenesis: differences in sequence and

timing of early developmental events. J Exp Zool 288: 352-365.

CHULIVER M & FABREZI M. 2019. A developmental staging table for *Physalaemus biligonigerus* (Cope, 1861) (Anura: Leptodactylidae). South Am J Herpetol 14: 150-161.

DUPORT-BRU AS, PONSSA ML & VERA CANDIOTI F. 2019. Postmetamorphic ontogenetic allometry and the evolution of skull shape in Nest-building frogs *Leptodactylus* (Anura: Leptodactylidae). Evol Dev 21: 265-277.

ESQUERRÉ D, SHERRATT E & KEOGH JS. 2017. Evolution of extreme ontogenetic allometric diversity and heterochrony in pythons, a clade of giant and dwarf snakes. Evolution 71: 2829-2844.

FROST DR. 2023. Amphibian Species of the World: an Online Reference. Version 6.1 March 20, 2023). Electronic Database accessible at https://amphibiansoftheworld.amnh.org/index.php. American Museum of Natural History, New York, USA. doi.org/10.5531/db.vz.0001.

GÓMEZ ML, ZARACHO VH & SANDOVAL MT. 2016. Desarrollo embrionario-larval y metamorfosis de *Physalaemus albonotatus* (Anura: Leptodactylidae). Rev Vet 27: 21-27.

GOSNER KL. 1960. A simplified table for staging anuran embryos and larvae with notes on identification. Herpetologica 16: 183-190.

GOULD SJ. 1966. Allometry and size in ontogeny and phylogeny. Biol Rev 41: 587-640.

GOULD SJ. 1977. Ontogeny and phylogeny. Cambridge, MA: Harvard University Press, 520 p.

GROSSO J, BALDO D, CARDOZO D, KOLENC F, BORTEIRO C, OLIVEIRA MIR, BONINO MF, BARRASSO DA & VERA CANDIOTI F. 2019. Early ontogeny and sequence heterochronies in Leiuperinae frogs (Anura: Leptodactylidae). PLoS ONE 14(6): e0218733.

GROSSO JR, BALDO D & VERA CANDIOTI F. 2017. Heterochronic changes during embryonic development of neotropical foam nesting frogs (genus *Leptodactylus*). Zool Anz 266: 35-49.

HADDAD CFB & POMBAL JP. 1998. Redescription of *Physalaemus spiniger* (Anura: Leptodactylidae) and description of two new reproductive modes. J Herpetol 32: 557-565.

HADDAD CFB & PRADO CPA. 2005. Reproductive modes in frogs and their unexpected diversity in the Atlantic forest of Brazil. Bioscience 55: 207-217.

KLINGENBERG CP. 1998. Heterochrony and allometry: The analysis of evolutionary change in ontogeny. Biol Rev 73: 79-123.

KLINGENBERG CP. 2011. MorphoJ: An integrated software package for geometric morphometrics. Mol Ecol Resour 11: 353-357.

KLINGENBERG CP. 2016. Size, shape, and form: concepts of allometry in geometric morphometrics. Dev Genes Evol 226: 113-137.

KLINGENBERG CP, DEBAT V & ROFF DA. 2010. Quantitative genetics of shape in cricket wings: Developmental integration in a functional structure. Evolution 64: 2935-2951.

LARSON PM. 2002. Chondrocranial development in larval *Rana sylvatica* (Anura: Ranidae): Morphometric analysis of cranial allometry and ontogenetic shape change. J Morphol 252: 131-144.

LARSON PM. 2004. Chondrocranial morphology and ontogenetic allometry in larval *Bufo americanus* (Anura, Bufonidae). Zoomorphology 123: 95-106.

LARSON PM. 2005. Ontogeny, phylogeny, and morphology in anuran larvae: morphometric analysis of cranial development and evolution in *Rana* tadpoles (Anura: Ranidae). J Morphol 264: 34-52.

LIMA MSCS & PEDERASSI J. 2012. Morphometrics and ratio of body proportionality of tadpoles of *Rhinella icterica* (Anura, Bufonidae) at different developmental stages. Br J Biol 72: 623-629.

LOURENÇO LB, TARGUETA C, BALDO D, NASCIMENTO J, GARCIA PC & ANDRADE G. 2015. Phylogeny of frogs from the genus *Physalaemus* (Anura, Leptodactylidae) inferred from mitochondrial and nuclear gene sequences. Mol Phylogenet Evol 92: 204-216.

MANEYRO R, NÚÑEZ D, BORTEIRO C, TEDROS M & KOLENC F. 2008. Advertisement call and female sexual cycle in Uruguayan populations of *Physalaemus henselii* (Anura, Leiuperidae). Iheringia Ser Zool 98: 210-214.

MITTEROECKER P, GUNZ P, WINDHAGER S & SCHAEFER K. 2013. A brief review of shape, form, and allometry in geometric morphometrics, with applications to human facial morphology. Hystrix 24: 59-66.

NASCIMENTO J, LIMA JD, SUÁREZ P, BALDO D, ANDRADE GV, PIERSON TW, FITZPATRICK BM, HADDAD CFB, RECCO-PIMENTEL SM & LOURENÇO LB. 2019 Extensive cryptic diversity within the *Physalaemus cuvieri – Physalaemus ephippifer* species complex (Amphibia, Anura) revealed by cytogenetic, mitochondrial, and genomic markers. Front Genet 10: 719.

NAVARRO ACOSTA G & VERA CANDIOTI MF. 2017. Alometría y heterocronías durante el desarrollo temprano de cinco

especies de *Hypsiboas* (Anura: Hylidae). Cuad Herpetol 31: 11-22.

OLIVEIRA MIRR, GROSSO J, NAPOLI MF, WEBER LN & VERA CANDIOTI F. 2022. Embryonic morphology in two species of the *Physalaemus signifer* clade (Anura: Leptodactylidae). Herpetol J 32: 85-92.

PIMENTA BVS, CRUZ CAG & SILVANO LS. 2005. A new species of the genus *Physalaemus* Fitzinger, 1826 (Anura, Leptodactylidae) from the Atlantic Rain Forest of southern Bahia, Brazil. Amphibia-Reptilia 26: 201-210.

PONSSA ML & VERA CANDIOTI MF. 2012. Patterns of skull development in anurans: Size and shape relationship during postmetamorphic cranial ontogeny in five species of the *Leptodactylus fuscus* group (Anura: Leptodactylidae). Zoomorphology 131: 349-362.

PUPIN NC, GASPARINI JL, BASTOS RG, HADDAD CFB & PRADO CPA. 2010. Reproductive biology of an endemic *Physalaemus* of the Brazilian Atlantic forest, and the trade-off between clutch and egg size in terrestrial breeders of the *P. signifer* group. Herpetol J 20: 147-156.

PUPIN NC, HADDAD CFB & PRADO CPA. 2018. Maternal provisioning by foam-nesting frogs of the genus *Physalaemus* (Anura, Leptodactylidae) in contrasting environments. Amphibia-Reptilia 39: 120-125.

QUINDERÉ YRD, LOURENÇO LB, ANDRADE GV, TOMATIS C, BALDO D & RECCO-PIMENTEL SM. 2009. Polytypic and polymorphic NOR variations in the widespread anuran *Physalaemus cuvieri* (Anura, Leiuperidae). Biol Res 42: 79-92.

RICHARDSON MK, HANKEN J, GOONERATNE ML, PIEAU C, RAYNAUD A, SELWOOD L & WRIGHT GM. 1997. There is no highly conserved embryonic stage in the vertebrates: implications for current theories of evolution and development. Anat Embryol 196: 91-106.

ROHLF FJ. 2005. tpsDig2, Version 2.04, Copyright © 2005. Ecology and Evolution, Suny at Stony Brook. Available in: http://life.bio.sunysb.edu/morph/soft-tps.html.

ROHLF FJ & BOOKSTEIN FL. 1990. Proceedings of the Michigan Morphometrics Workshop. Special Publication No. 2, University of Michigan Museum of Zoology: Ann Arbor, 380 p.

RUGGERI JG & WEBER LN. 2012. A survey of the internal oral features and external morphology of *Physalaemus* larvae (Anura, Leptodactylidae). Zootaxa 3200: 1-26.

SALICA MJ, HAAD MB, VERA CANDIOTI F & FAIVOVICH J. 2011. Early development of two species of *Phyllomedusa* (Anura: Phyllomedusinae). Salamandra 47: 144-154.

SALTHE SN & DUELLMAN WE. 1973. Quantitative constraints associated with reproductive mode in anurans. In: Vial JL (Ed), Evolutionary biology of the anurans, Columbia: University of Missouri Press, p. 229-249.

SMITH KK. 2001. Heterochrony revisited: the evolution of developmental sequences. Biol J Linn Soc Lond 73: 169-186.

STRELIN MM, BENITEZ-VIEYRA S, FORNONI J, KLINGENBERG CP & COCUCCI A. 2016. Exploring the ontogenetic scaling hypothesis during the diversification of pollination syndromes in *Caiophora* (Loasaceae, subfam. Loasoideae). Ann Bot 117: 937-947.

VERA CANDIOTI F ET AL. 2016. Structural and heterochronic variations during the early ontogeny in toads (Anura: Bufonidae). Herpetol Monogr 30: 79-118.

VERA CANDIOTI MF, HAAD B, BALDO D, KOLENC F, BORTEIRO C & ALTIG R. 2011. Different pathways are involved in the early development of the transient oral apparatus in anuran tadpoles (Anura: Leiuperidae). Biol J Linn Soc 104: 330-345.

VIEIRA WLDS & ARZABE C. 2008. Description of the tadpole of *Physalaemus cicada* (Anura, Leiuperidae). Iheringia Ser Zool 98: 266-269.

WEBER LN & CARVALHO-E-SILVA SP. 2001. Descrição da larva de *Physalaemus signifer* (Girard, 1853) (Amphibia, Anura, Leptodactylidae) e informações sobre a reprodução e a distribuição geográfica da espécie. Bol Mus Nac NS Zool 462: 1-6.

WILSON LAB & SÁNCHEZ-VILLAGRA MR. 2009. Diversity trends and their ontogenetic basis: An exploration of allometric disparity in rodents. Proc R Soc B Biol Sci 277: 1227-1234.

SUPPLEMENTARY MATERIAL

Figure S1.
Table SI.

How to cite

OLIVEIRA MIRR, GROSSO J, NAPOLI MF, WEBER LN & VERA CANDIOTI F. 2024. Patterns of allometric and heterochronic changes in the early ontogeny of species of *Physalaemus* (Anura: Leptodactylidae). An Acad Bras Cienc 96: e20231231. DOI 10.1590/0001-3765202420231231.

Manuscript received on November 28, 2023;
accepted for publication on May 11, 2024

MARIANNA ISABELLA R.R. DE OLIVEIRA[1]
https://orcid.org/0000-0003-2149-6095

JIMENA GROSSO[2,3,4]
https://orcid.org/0000-0002-1897-6621

MARCELO F. NAPOLI[1]
https://orcid.org/0000-0003-3843-0543

LUIZ N. WEBER[1,5]
https://orcid.org/0000-0001-6639-1022

FLORENCIA VERA CANDIOTI[2]
https://orcid.org/0000-0002-6133-9951

[1]Universidade Federal da Bahia, Programa de Pós-Graduação em Biodiversidade e Evolução, Instituto de Biologia, Campus Universitário de Ondina, Rua Barão de Jeremoabo, s/n, Ondina, 40170-115 Salvador, BA, Brazil

[2]Unidad Ejecutora Lillo – CONICET-FML, Miguel Lillo 251, 4000 San Miguel de Tucumán, Argentina

[3]Instituto de Ciencias Marinas y Limnológicas, Universidad Austral de Chile, Independencia 631, 5090000 Valdivia, Chile

[4]Centro de Humedales Río Cruces (UACh), Independencia 631, 5090000 Valdivia, Chile

[5]Universidade Federal do Sul da Bahia, Centro de Formação em Ciências Ambientais, BR 367, Rodovia Porto Seguro-Eunápolis, Km 10, 45810-000 Porto Seguro, BA, Brazil

Correspondence to: **Marianna Isabella Rosa Rodrigues de Oliveira**
E-mail: oliveira.rmi@gmail.com

Author contributions

MARIANNA ISABELLA R. R. DE OLIVEIRA: conceptualization; formal analysis; investigation; methodology; project administration; writing-original draft; writing review & editing. JIMENA GROSSO: methodology; investigation; writing review & editing. MARCELO F. NAPOLI: supervision; writing review & editing. LUIZ N. WEBER: conceptualization; formal analysis; methodology; resources; supervision; writing the original draft. FLORENCIA VERA CANDIOTI: conceptualization; formal analysis; investigation; methodology; supervision; writing-original draft; writing review & editing.